

On the Robot Compliant Motion Control

H. Kazerooni

Mechanical Engineering Department,
University of Minnesota,
Minneapolis, Minn. 55455

The work presented here is a nonlinear approach for the control and stability analysis of manipulative systems in compliant maneuvers. Stability of the environment and the manipulator taken as a whole has been investigated using unstructured models for the dynamic behavior of the robot manipulator and the environment, and a bound for stable manipulation has been derived. We show that for stability of the robot, there must be some initial compliancy either in the robot or in the environment. The general stability condition has been extended to the particular case where the environment is very rigid in comparison with the robot stiffness. A fast, light-weight, active end-effector (a miniature robot) which can be attached to the end-point of large commercial robots has been designed and built to verify the control method. The device is a planar, five-bar linkage which is driven by two direct drive, brush-less DC motors. The control method makes the end-effector to behave dynamically as a two-dimensional, Remote Center Compliance (RCC).

1 Introduction

Most assembly operations and manufacturing tasks require mechanical interactions with the environment or with the object being manipulated, along with "fast" motion in unconstrained space. In constrained maneuvers, the interaction force¹ must be accommodated rather than resisted. Two methods have been suggested for development of compliant motion. The first approach is aimed at controlling force and position in a nonconflicting way [10, 11, 12, 18]. In this method, force is commanded along those directions constrained by the environment, while position is commanded along those directions in which the manipulator is unconstrained and free to move. The second approach is focused on developing a relationship between the interaction force and the manipulator position [1, 4, 5, 13]. By controlling the manipulator position and specifying its relationship with the interaction force, a designer can ensure that the manipulator will be able to maneuver in a constrained space while maintaining appropriate contact force. This paper describes an analysis on the control and stability of the robot in constrained maneuvers when the second method is employed to control the robot compliancy.

We start with modeling the robot and the environment with unstructured dynamic models. To arrive at a general stability criterion, we avoid using structured dynamic models such as first or second order transfer functions as general representations of the dynamic behavior of the components of the robot (such as actuators). Using unstructured models for the robot and environment, we analyze the stability of the robot and environment via the Small Gain Theorem and Nyquist Criterion. We show that the stability criterion achieved via the Nyquist

method is a subclass of the condition given by the Small Gain Theorem. For a particular application, one can replace the unstructured dynamic models with known models and then a tighter condition can be achieved. The stability criterion reveals that there must be some initial compliancy either in the robot or in the environment. The initial compliancy in the robot can be obtained by a passive compliant element such as an RCC (Remote Center Compliance) or compliancy within the positioning feedback. Practitioners always observed that the system of a robot and a stiff environment can always be stabilized when a compliant element (e.g., piece of rubber or an RCC) is installed between the robot and environment. The stability criterion also shows that no compensator can be found to stabilize the interaction of the ideal positioning system (very rigid tracking robot) with an infinitely rigid environment. In this case the robot and environment both resemble ideal sources of flow (defined in bond graph theory) and they do not physically complement each other. A fast, light-weight, active end-effector (a miniature robot) which can be attached to the end-point of a commercial robot manipulator has been designed and built to experimentally verify the control method.

2 Dynamic Model of the Robot With Positioning Controllers

In this section, a general approach will be developed to describe the dynamic behavior of a large class of industrial and research robot manipulators having positioning (tracking) controllers. The fact that most industrial manipulators already have some kind of positioning controller is the motivation behind our approach. Also, a number of methodologies exist for the development of robust positioning controllers for direct and nondirect robot manipulators [14, 17].

In general, the end-point position of a robot manipulator that has a positioning controller is a dynamic function of its

¹In this article, "force" implies force and torque and "position" implies position and orientation.

Contributed by the Dynamic Systems and Control Division for publication in the JOURNAL OF DYNAMIC SYSTEMS, MEASUREMENT, AND CONTROL. Manuscript received by the Dynamic Systems and Control Division February 1987; revised manuscript received May 2, 1988. Associate Editor: R. Shoureshi.

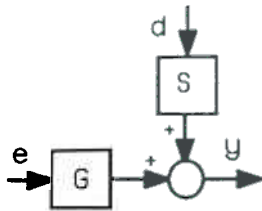


Fig. 1 The dynamics of the manipulator with the positioning controller (all the operators of the block diagrams of this paper are unspecified and may be transfer function matrices or time domain input-output relationships)

input trajectory vector, e , and the external force, d . Let G and S be two functions that show the robot end-point position in a global coordinate frame, y , is a function of the input trajectory, e , and the external force, d .² (d is measured in the global coordinate frame also.)

$$y = G(e) + S(d) \quad (1)$$

The motion of the robot end-point in response to imposed forces, d , is caused by either structural compliance in the robot³ or by the compliance of the positioning controller. Robot manipulators with tracking controllers are not infinitely stiff in response to external forces (also called disturbances). Even though the positioning controllers of robots are usually designed to follow the trajectory commands and reject disturbances, the robot end-point will move somewhat in response to imposed forces on it. S is called the sensitivity function and it maps the external forces to the robot end-point position. For a robot with a "good" positioning controller, S is a mapping

²The assumption that linear superposition (in equation (1)) holds for the effects of d and e is useful in understanding the nature of the interaction between the robot and the environment. This interaction is in a feedback form and will be clarified with the help of Fig. 2. We will note in Section 4 that the results of the nonlinear analysis do not depend on this assumption, and one can extend the obtained results to cover the case when $G(e)$ and $S(d)$ do not superimpose.

³In a simple example, if a Remote Center Compliance (RCC) with a linear dynamic behavior is installed at the endpoint of the robot, then S is equal to the reciprocal of stiffness (impedance in the dynamic sense) of the RCC.

with small gain. (The gain of an operator is defined in Appendix A.) No assumption on the internal structures of $G(e)$ and $S(d)$ is made. Figure 1 shows the nature of the mapping in equation (1).

We define $G(e)$ and $S(d)$ as stable, nonlinear operations in L_p -space to represent the dynamic behavior of the closed-loop robots. $G(e)$ and $S(d)$ are such that $G: L_p^n \rightarrow L_p^n$, $S: L_p^n \rightarrow L_p^n$ and also there exist constants α_1 , β_1 , α_2 , and β_2 such that $\|G(e)\|_p \leq \alpha_1 \|e\|_p + \beta_1$ and $\|S(d)\|_p \leq \alpha_2 \|d\|_p + \beta_2$. (The definition of stability in L_p -sense is given in Appendix A.)

A similar modeling method can be given for the analysis of the linearly treated robots.⁵ The transfer function matrices, G and S in equation (2) are defined to describe the dynamic behavior of a linearly treated robot manipulator with positioning controller.

$$y(j\omega) = G(j\omega)e(j\omega) + S(j\omega)d(j\omega) \quad (2)$$

In equation (2), S is called the sensitivity transfer function matrix and it maps the external forces to the end-point position. $G(j\omega)$ is the closed-loop transfer function matrix that maps the input trajectory vector, e , to the robot end-point position, y . For a robot with a "good" positioning controller, within the closed loop bandwidth; $S(j\omega)$ is "small" in the singular value sense,⁶ while $G(j\omega)$ is approximately a unity matrix.

3 Dynamic Behavior of the Environment

The environment can be very "soft" or very "stiff." We do

⁵Throughout this paper, for the benefit of clarity, we develop the frequency domain theory for linearly treated robots in parallel with the nonlinear analysis. The linear analysis is useful not only for analysis of robots with inherently linear dynamics, but also for robots with locally linearized dynamic behavior. In the latter case, the analysis is correct only in the neighborhood of the operating point.

⁶The maximum singular value of a matrix A , $\sigma_{\max}(A)$ is defined as:

$$\sigma_{\max}(A) = \max \frac{|Az|}{|z|}$$

where z is a nonzero vector and $| \cdot |$ denotes the Euclidean norm of a vector or a scalar.

Nomenclature

A = the closed-loop mapping from r to e in Fig. 4	j = complex number notation $\sqrt{-1}$	ment position before contact
d = vector ⁴ of the external force on the robot end-point	J_c = Jacobian	θ = vector of the joint angles of the robot
e = input trajectory vector	l_i, m_i = length and mass of each link	τ = vector of the robot torques
E = environment dynamics	M_0 = inertia matrix	$\epsilon_e, \epsilon_d, \mu, \gamma$ = positive scalars
f = vector of the contact force, $(f_1, f_2, \dots, f_n)^T$	r = input-command vector	ω_0 = frequency range of operation (bandwidth)
f_∞ = the limiting value of the contact force for infinitely rigid environment	n = degrees of the freedom of the robot $n \leq 6$	α_i, β_i, ν = positive scalars
G = robot dynamics with positioning controller	S = robot manipulator sensitivity (1/stiffness)	α = small perturbation of θ_n in the neighborhood of $\theta_n = 90$ deg
H = compensator (operating on the contact force, f)	T = positive scalar	δe = end-point deflection in y_n -direction
I_n = identity matrix	V = the forward loop mapping from e to f in Fig. 4	$\delta y_n, \delta y_t$ = end-point deflection in the direction normal and tangential to the part
j_i = moment of inertia of each link relative to the end-point of the link	x = vector of the environment deflection	$\delta f_n, \delta f_t$ = contact force in the direction normal and tangential to the part
	x_i = location of the center of mass	ω_d = dynamic manipulability
	y = vector of the robot end-point position	
	y_∞ = the limiting value of the robot position for rigid environment	
	x_0 = vector of the environ-	

⁴All vectors in this paper are $n \times 1$ vectors.

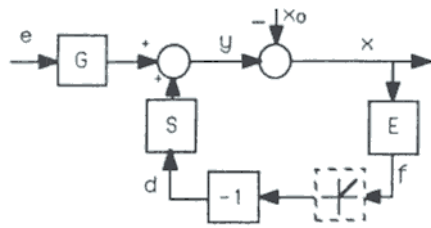


Fig. 2 Interaction of the robot manipulator with the environment

not restrain ourselves to any geometry or to any structure. If one point on the environment is displaced as vector of x , with force vector, f , then the dynamic behavior of the environment is given by equation (3).

$$f = E(x) \quad (3)$$

If x_0 is the initial location of the point of contact on the environment before deformation occurs then, $x = y - x_0$. E is assumed to be stable in L_p -sense; $E: L_p^n \rightarrow L_p^n$ and $\|E(x)\|_p \leq \alpha_3 \|x\|_p + \beta_3$. Confining equation (3) to cover the linearly treated environment, equation (4) represents the dynamic behavior of the environment.

$$f(j\omega) = E(j\omega)x(j\omega) \quad (4)$$

$E(j\omega)$ is a transfer function matrix that maps the displacement vector, x , to the contact force, f . Matrix E is a $n \times n$ transfer function matrix. E is a singular matrix when the robot interacts with the environment in only some directions. For example, in grinding a surface, the robot is constrained by the environment in the direction normal to the surface only. Readers can be convinced of the truth of equation (4) by analyzing the relationship of the force and displacement of a mass, spring and damper as a simple model of the environment. E resembles the impedance of a system. References [4 and 5] represent $(Js^2 + Ds + K)$ for E where J , D , and K are symmetric matrices and $s = j\omega$ (4).

4 Nonlinear Dynamic Behavior of the Robot and Environment

Suppose a manipulator with dynamic equation (1) is in contact with an environment given by equation (3); then $f = -d$. Figure 2 shows the dynamics of the robot manipulator and environment when they are in contact with each other. Note that in some applications, the robot will have only unidirectional force on the environment. For example, in the grinding a surface by a robot, the robot can only push the surface. If one considers positive f_i for "pushing" and negative f_i for "pulling," then in this class of manipulation, the robot manipulator and the environment are in contact with each other only along those directions where $f_i > 0$ for $i = 1, \dots, n$. In some applications such as screwing a bolt, the interaction force can be positive and negative. This means the robot can have clockwise and counterclockwise interaction torque. The nonlinear discriminator block diagram in Fig. 2 is drawn with dashed-line to illustrate the above concept.

Using equations (1) and (3), equations (5) and (6) represent the entire dynamic behavior of the robot and environment taken as a whole.

$$y = G(e) + S(-f) \quad (5)$$

$$f = E(x) \quad \text{where } x = y - x_0 \quad (6)$$

If all the operators in Fig. 2 are considered linear transfer function matrices, equations (7) and (8) can be obtained to represent the end point position and the contact force when $x_0 = 0$.

$$y = (I_n + S E)^{-1} G e \quad (7)$$

$$f = E(I_n + S E)^{-1} G e \quad (8)$$

To simplify the block diagram of Fig. 2, we introduce a mapping from e to f .

$$f = V(e) \quad (9)$$

If all the operators in Fig. 2 are transfer function matrices, then $V = E(I_n + S E)^{-1} G$. V is assumed to be a stable operator in L_p -sense; therefore $V: L_p^n \rightarrow L_p^n$ and also $\|V(e)\|_p \leq \alpha_4 \|e\|_p + \beta_4$. With this assumption, we basically claim that a robot with stable tracking controller remains stable when it is in contact with an environment. Note that one can still define V without assuming the superposition of effects of e and d in equation (5) (or equation (1)).

5 The Architecture of the Closed-Loop System

We propose the architecture of Fig. 3 to develop compliancy for the robot. The compensator, H , is considered to operate on the contact force, f . The compensator output signal is being subtracted from the input command vector, e , resulting in the input trajectory vector, r , for the robot manipulator. The readers should be reminded that the robot in Fig. 3 can be considered a weak tracking robot (open loop robot without any feedback on the position and velocity) when the gain of S is a large number.

There are two feedback loops in the system; the inner loop (which is the natural feedback loop), is the same as the one shown in Fig. 2. This loop shows how the contact force affects the robot in a natural way when the robot is in contact with the environment. The outer feedback loop is the controlled feedback loop. If the robot and the environment are not in contact, then the dynamic behavior of the system reduces to the one represented by equation (1) (with $d = 0$), which is a plain positioning system. When the robot and the environment are in contact, then the values of the contact force and the end-point position of robot are given by f and y where the following equations are true:

$$y = G(e) + S(-f) \quad (10)$$

$$f = E(x) \quad \text{where } x = y - x_0 \quad (11)$$

$$e = r - H(f) \quad (12)$$

If the operators in equations (10), (11), and (12) are considered as transfer function matrices, equations (13) and (14) can be obtained to represent the interaction force and the robot end-point position for linearly treated systems when $x_0 = 0$.

$$f = E(I_n + S E + G H E)^{-1} G r \quad (13)$$

$$y = (I_n + S E + G H E)^{-1} G r \quad (14)$$

The objective is to choose a class of compensators, H , to control the contact force with the input command r . By knowing S , G , E , and choosing H , one can shape the contact force. The value of H is the choice of designer and, depending on the task, it can have various values in different directions. A large value for H develops a compliant robot while a small H generates a stiff robot. Reference [7] describes a micro manipulator in which the compliancy in the system is shaped for metal removal application. Note that S and GH add in equation (13) to develop the total compliancy in the system. GH represents the electronic compliancy in the robot while S models the natural hardware compliancy (such as RCC or the robot structural compliancy) in the system.⁷ Equation (13) also shows that a robot with good tracking capability (small

⁷Equation (13) can be rewritten as $f = (E^{-1} + S + GH)^{-1} G r$. Note that the environment admittance (1/impedance in the linear domain), E^{-1} , the robot sensitivity (1/stiffness in the linear domain), S , and the electronic compliancy, GH , add together to form the total sensitivity of the system. If $H = 0$, then only the admittance of the environment and the robot add together to form the compliancy for the system. By closing the loop via H , one can not only add to the total sensitivity but also shape the sensitivity of the system.

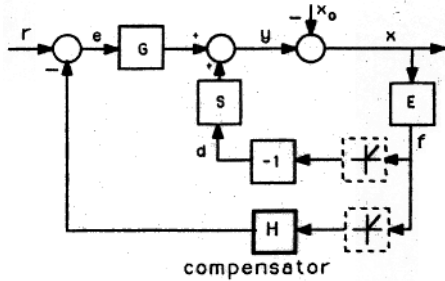


Fig. 3 The closed-loop system

gain for S) may generate a large contact force in a particular contact. One cannot choose arbitrarily large values for H ; the stability of the closed-loop system of Fig. 3 must be guaranteed. The trade-off between the closed-loop stability and the size of H is investigated in Section 6.

When the robot is not in contact with the environment (i.e., the outer feedback loops in Fig. 3 do not exist), the actual position of the robot end-point is governed by equation (1) (with $d=0$). When the robot is in contact with the environment, then the contact force follows r according to equations (10), (11), and (12). The input command vector, r , is used differently for the two categories of maneuverings; as an input trajectory command in unconstrained space (equation (1) with $d=0$) and as a command to control force in constrained space. There is no hardware or software switch in the control system when the robot travels between unconstrained space and constrained space. The feedback loop on the contact force closes naturally when the robot encounters the environment.

6 Stability Analysis

The objective of this section is to arrive at a sufficient condition for stability of the system shown in Fig. 3. This sufficient condition leads to the introduction of a class of compensators, H , that can be used to develop compliancy for the family of robot manipulators with dynamic behavior represented by equation (1). Using operator V defined by equation (9), the block diagram of Fig. 4 is constructed as a simplified version of the block diagram in Fig. 3. First we use the Small Gain Theorem to derive the general stability condition. Then, with the help of a corollary, we show the stability condition when H is chosen as a linear operator (transfer function matrix) while V is a nonlinear operator. Finally, if all the operators in Fig. 3 are transfer function matrices, then the stability bound is shown by inequality 25. Section 7 is devoted to stability analysis of the linearly treated systems,⁸ when the environment is infinitely rigid in comparison with the robot stiffness.

The following proposition (using the Small Gain Theorem in references [15, 16]) states the stability condition of the closed-loop system shown in Fig. 4.

If conditions I, II, and III hold:

I. V is a L_p -stable operator, that is

$$(a) V(e): L_p^n \rightarrow L_p^n \quad (15)$$

$$(b) \|V(e)\|_p \leq \alpha_4 \|e\|_p + \beta_4 \quad (16)$$

II. H is chosen such that mapping $H(f)$ is L_p -stable, that is

$$(a) H(f): L_p^n \rightarrow L_p^n \quad (17)$$

$$(b) \|H(f)\|_p \leq \alpha_5 \|f\|_p + \beta_5 \quad (18)$$

III. and $\alpha_4 \alpha_5 < 1$ (19)

then the closed-loop system (Fig. 4) is L_p -stable. The proof is

⁸The stability analysis and the role of robot sensitivity and environment dynamics on size H are best shown by linear theory in equations (27)–(31). In particular, we confine our analysis to linear one-degree-of-freedom robot in equations (32) and (33) for better understanding the nature of the stability analysis.

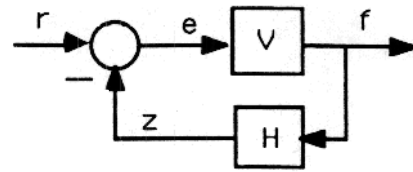


Fig. 4 Simplified version of Fig. 3. In the linear domain, $V = E(SE + I_n)^{-1}G$.

given in Appendix A. Substituting for $\|f\|_p$ from inequality 16 into inequality 18 results in inequality 20. (Note that $f = V(e)$)

$$\|H(V(e))\|_p \leq \alpha_4 \alpha_5 \|e\|_p + \alpha_5 \beta_4 + \beta_5 \quad (20)$$

$\alpha_4 \alpha_5$ in inequality 20 represents the gain of the loop mapping, $H(V(e))$. The third stability condition requires that H be chosen such that the loop mapping, $H(V(e))$, is linearly bounded with less than a unity slope. The following corollary develops a stability bound if H is selected as a linear transfer function matrix.

Corollary. The key parameter in the proposition is the size of $\alpha_4 \alpha_5$. According to the proposition, to guarantee the stability of the system, H must be chosen such that norm of $HV(e)$ is linearly bounded with a slope that is smaller than unity. If H is chosen as a linear operator (the impulse response) while all the other operators are still nonlinear, then:

$$\|HV(e)\|_p \leq \gamma \|V(e)\|_p \quad (21)$$

where: $\gamma = \sigma_{\max}(N)$ (22)

σ_{\max} indicates the maximum singular value, and N is a matrix whose ij th entry is $\|H_{ij}\|_1$. In other words, each member of N is the L_1 norm of each corresponding member of H . Considering inequality 16, inequality 21 can be rewritten as:

$$\|HV(e)\|_p \leq \gamma \|V(e)\|_p \leq \gamma \alpha_4 \|e\|_p + \gamma \beta_4 \quad (23)$$

Comparing inequality 23 with inequality 20, to guarantee the closed loop stability, $\gamma \alpha_4$ must be smaller than unity, or, equivalently:

$$\gamma < \frac{1}{\alpha_4} \quad (24)$$

To guarantee the stability of the closed-loop system, H must be chosen such its "size" is smaller than the reciprocal of the "gain" of the forward loop mapping in Fig. 4. Note that γ represents a "size" of H in the singular value sense.

When all the operators of Fig. 4 are linear transfer function matrices one can use Multivariable Nyquist Criterion (9) to arrive at the sufficient condition for stability of the closed loop system. This sufficient condition leads to the introduction of a class of transfer function matrices, H , that stabilize the family of linearly treated robot manipulators and environment using dynamic equations (2) and (4). The detailed derivation for the stability condition is given in Appendix C. Appendix D shows that the stability condition given by Nyquist Criterion is a subset of the condition given by the Small Gain Theorem. According to the results of Appendix C, the sufficient condition for stability is given by inequality 25.

$$\sigma_{\max}(GHE) < \sigma_{\min}(SE + I_n) \quad \text{for all } \omega \in (0, \infty) \quad (25)$$

or a more conservative condition,

$$\sigma_{\max}(H) < \frac{1}{\sigma_{\max}(E(I_n + SE)^{-1}G)} \quad \text{for all } \omega \in (0, \infty) \quad (26)$$

Similar to the nonlinear case, H must be chosen such that its "size" is smaller than the reciprocal of the "size" of the forward loop mapping in Fig. 4 to guarantee the stability of the closed-loop system. Note that in inequality 26 σ_{\max} represents a "size" of H in the singular value sense. Consider $n=1$ (one degree of freedom system) for more understanding about the

stability criterion. The stability criterion when $n = 1$ is given by inequality 27.

$$|HG| < |(S + 1/E)| \quad \text{for all } \omega \in (0, \infty) \quad (27)$$

where $| \cdot |$ denotes the magnitude of a transfer function. Since in many cases $G \approx 1$ for all $0 \leq \omega \leq \omega_0$, then H must be chosen such that:

$$|H| < |(S + 1/E)| \quad \text{for all } \omega \in (0, \omega_0) \quad (28)$$

Inequality 28 reveals some facts about the size of H . The smaller the sensitivity of the robot manipulator is, the smaller H must be chosen. Also the inequality 28, the more rigid the environment is, the smaller H must be chosen. In the "ideal case," no H can be found to allow a perfect positioning system ($S = 0$) to interact with an infinitely rigid environment ($E = \infty$). In other words, for stability of the system shown in Fig. 3, there must be some compliancy either in robot or in the environment. RCC, structural dynamics and the tracking controller stiffness form the compliancy on the robot. Section 7 gives more information about the effects of E on the stability region.

7 Stability for Very Rigid Environment

In most manufacturing tasks, the end-point of the robot manipulator is in contact with a very stiff environment. Robotic deburring and grinding are examples of practical tasks in which the robot is in contact with stiff environment [6, 7]. According to the results in Appendix B, when the environment is very stiff, (E is very "large" in the singular value sense), the limiting values for the contact force and the end-point position are given by equations (29) and (30), respectively:

$$f_\infty = (S + GH)^{-1} G r \quad (29)$$

$$y_\infty = 0 \quad (30)$$

Since $G \approx I_n$ for all $\omega \in (0, \omega_0)$, (the end-point position is "approximately" equal to the input trajectory vector, e), the value of the contact force, f , within the bandwidth of the system ($0, \omega_0$) can be approximated by equation (31):

$$f_\infty \approx (S + H)^{-1} r \quad \text{for all } \omega \in (0, \omega_0) \quad (31)$$

By knowing S and choosing H , one can shape the contact force. The value of $(S + H)$ within $(0, \omega_0)$ is the designer's choice and, depending on the task, it can have various values in different directions (3). A large value for $(S + H)$ within $(0, \omega_0)$ develops a compliant system while a small $(S + H)$ generates a stiff system. If H is chosen such that $(S + H)$ is "large" in the singular value sense at high frequencies, then the contact force in response to high frequency components of r will be small. If H is chosen to guarantee the compliance in the system according to equation (29), then it must also satisfy the stability condition. It can be shown that the stability criterion for interaction with a very rigid environment is given by inequality 32:

$$\sigma_{\max}(H) < \frac{1}{\sigma_{\max}(S^{-1}G)} \quad \text{for all } \omega \in (0, \infty) \quad (32)$$

It is clear that if the environment is very rigid, then one must choose a very small H to satisfy the stability of the system when S is "small." (A good positioning system has "small" S .) Since $G \approx I_n$ for all $\omega \in (0, \omega_0)$, the bound for H , for a rigid environment and a "small" stiffness, is given by inequality 33.

$$\sigma_{\max}(H) < \sigma_{\min}(S) \quad \text{for all } \omega \in (0, \omega_0) \quad (33)$$

If S is zero, then no H can be obtained to stabilize the system. To stabilize the system of the very rigid environment and the robot, there must be a minimum compliancy in the robot. Direct drive manipulators, because of the elimination of the transmission systems, often have large S . This allows for a wider stability range in constrained manipulation.

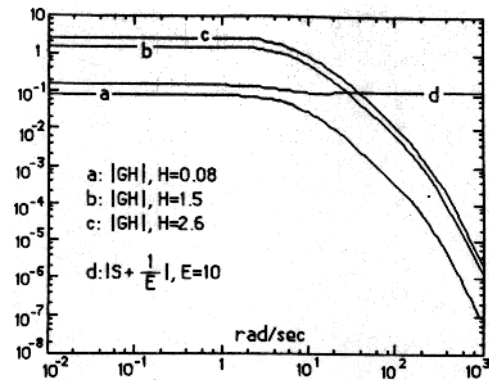


Fig. 5 $|S + 1/E|$ and $|GH|$ for soft environment

We conclude that for stability of the environment and robot taken as a whole, there must be some initial compliancy either in the robot or in the environment. The initial compliancy in the robot can be obtained by a nonzero sensitivity function or a passive compliant element such as an RCC. Practitioners always observed that the system of a robot and a stiff environment can always be stabilized when a compliant element (e.g., piece of rubber or an RCC) is installed between the robot and environment. One can also stabilize the system of robot and environment by increasing the robot sensitivity function. In many commercial manipulators the sensitivity of the robot manipulators can be increased by decreasing the gain of each actuator positioning loop. This also results in a narrower bandwidth (slow response in the unconstrained maneuvering) for the robot positioning system (2).

8 An Example on the Stability Criteria

Consider a one-degree-of-freedom robot with G and S in equation (1) given as:

$$G(S) = \frac{1}{(s/6 + 1)(s/10 + 1)(s/200 + 1)(s/250 + 1)(s/300 + 1)}$$

$$S(s) = \frac{.05}{(s/5 + 1)(s/9 + 1)}$$

The system has a good positioning capability (small gain for S and unity gain for G at DC). The poles that are located at -250 and -300 show the high frequency modes in the robot. The stability of this system when it is in contact with various environment dynamics is analyzed. We assume E is constant and has the value of 10 for all frequency ranges. If we consider H as a constant gain, then inequality 27 yields that for $H \leq 0.14$ the value of $|GH|$ is always smaller than $|S + 1/E|$ for all $\omega \in (0, \infty)$. Figure 5 shows the plots of $|GH|$ and $|S + 1/E|$ for three values of H . For $H = 0.08$ the system is stable with the closed-loop poles located at $(-301.59, -244.81, -204.27, -9.25, -5.35, -7.37 \pm 8.4j)$ while $H = 2.6$ results in unstable system with the closed-loop poles located at $(-324.9, -221.31 \pm 63.52j, 0.78 \pm 37.82j, -9.01, -5.02)$. Note that the stability condition derived with inequality 27 is a sufficient condition for stability; many compensators can be found to stabilize the system without satisfying inequality 27. Figure 5 shows an example ($H = 1.5$) that does not satisfy inequality 27 however the system is stable with closed-loop poles at $(-317.67, -221.66 \pm 49.06j, -2.48 \pm 29.9j, -9.02, -5.03)$. If one uses root locus for stability analysis, for $H \leq 2.32$ all the closed loop poles will be in the left half plane. Once a constant value for stabilizing H established, one can choose a dynamic compensator to filter out the high frequency noise in the force measurements:

$$H = \frac{0.08}{|s + 1|}$$

tain any spring or dampers. The compliancy in the active end-effector is developed electronically and therefore can be modulated by an on-line computer. Satisfying a kinematic constraint for this end-effector allows for uncoupled dynamic behavior for a bounded range. Two state-of-the-art miniature actuators power the end-effector directly. A miniature force cell measures the forces in two dimensions. The tool holder can maneuver a very light pneumatic grinder in a linear workspace of about 0.3×0.3 in. A bound for the global stability of the manipulator and environment has been derived. For stability of the environment and the robot taken as a whole, there must be some initial compliancy either in the robot or in the environment. The initial compliancy in the robot can be obtained by a nonzero sensitivity function for the positioning controller or a passive compliant element.

Acknowledgment

This research work is supported by the National Science Foundation grant under Contract NSF/DMC-8604123.

References

- Hogan, N., "Impedance Control: An Approach to Manipulation," ASME JOURNAL OF DYNAMIC SYSTEMS, MEASUREMENT, AND CONTROL, Vol. 107, 1985.
- Hollis, R. L., "A Planar XY Robotic Fine Positioning Device," IEEE International Conference on Robotics and Automation, St. Louis, MO, Mar. 1985.
- Kazerooni, H., and Houpt, P. K., "On The Loop Transfer Recovery," *Int. J. of Control*, Vol. 43, No. 3, Mar. 1986.
- Kazerooni, H., "Fundamentals of Robust Compliant Motion for Manipulators," *IEEE J. of Robotics and Automation*, Vol. 2, No. 2, June 1986.
- Kazerooni, H., "A Design Method for Robust Compliant Motion of Manipulators," *IEEE J. of Robotics and Automation*, Vol. 2, No. 2, June 1986.
- Kazerooni, "An Approach to Automated Deburring by Robot Manipulators," ASME JOURNAL OF DYNAMIC SYSTEMS, MEASUREMENT, AND CONTROL, Dec. 1986.
- Kazerooni, H., "Robotic Deburring of Parts with Unknown Geometry," *Proceedings of American Control Conference*, Atlanta, GA, June 1988.
- Kazerooni, H., "Direct Drive Active Compliant End-effector," *IEEE J. of Robotics and Automation*, Vol. 4, No. 3, June 1988.
- Lehtomaki, N. A., Sandell, N. R., and Athans, M., "Robustness Results in Linear-Quadratic Gaussian Based Multivariable Control Designs," *IEEE Trans. on Automatic Control*, Vol. 26, No. 1, Feb. 1981, pp. 75-92.
- Mason, M. T., "Compliance and Force Control for Computer Controlled Manipulators," *IEEE Transaction on Systems, Man, and Cybernetics*, SMC-11(6), June 1981, pp. 418-432.
- Paul, R. P. C., and Shimano, B., "Compliance and Control," *Proceedings of the Joint Automatic Control Conference*, San Francisco, 1976, pp. 694-699.
- Raibert, M. H., and Craig, J. J., "Hybrid Position/Force Control of Manipulators," ASME JOURNAL OF DYNAMIC SYSTEMS, MEASUREMENT, AND CONTROL, Vol. 102, June 1981, pp. 126-133.
- Salisbury, K. J., "Active Stiffness Control of Manipulator in Cartesian Coordinates," *Proceedings of the 19th IEEE Conference on Decision and Control*, pp. 95-100, IEEE, Albuquerque, N. Mex., Dec. 1980.
- Slotine, J. J., "The Robust Control of Robot Manipulators," *The International J. of Robotics Research*, Vol. 4, No. 2, 1985.
- Vidyasagar, M., *Nonlinear Systems Analysis*, Prentice-Hall, 1978.
- Vidyasagar, M., and Desoer, C. A., *Feedback Systems: Input-Output Properties*, Academic Press, 1975.
- Vidyasagar, M., Spong, M. W., "Robust Nonlinear Control of Robot Manipulators," IEEE Conference on Decision and Control, Dec. 1985.
- Whitney, D. E., "Force-Feedback Control of Manipulator Fine Motions," ASME JOURNAL OF DYNAMIC SYSTEMS, MEASUREMENT, AND CONTROL, June 1977, pp. 91-97.
- Yoshikawa, T., "Dynamic Manipulability of Robot Manipulators," *Journal of Robotic Systems*, Vol. 2, No. 1, 1985.

APPENDIX A

Definitions 1 to 7 will be used in the stability proof of the closed-loop system (Vidyasagar, 1978, Vidyasagar and Desoer, 1975).

Definition 1: For all $p \in (1, \infty)$, we label as L^p the set consisting of all functions $f = (f_1, f_2, \dots, f_n)^T: (0, \infty) \rightarrow R^n$ such that:

$$\int_0^\infty |f_i|^p dt < \infty \quad \text{for } i = 1, 2, \dots, n$$

Definition 2: For all $T \in (0, \infty)$, the function f_T defined by:

$$f_T = \begin{cases} f & 0 \leq t \leq T \\ 0 & T < t \end{cases}$$

is called the truncation of f to the interval $(0, T)$.

Definition 3: The set of all functions $f = (f_1, f_2, \dots, f_n)^T: ((0, \infty) \rightarrow R^n$ such that $f^T \in L^p$ for all finite T is denoted by L^p_{pe} . f by itself may or may not belong to L^p .

Definition 4: The norm on L^p is defined by:

$$\|f\|_p = \left[\sum_{i=1}^n \|f_i\|_p^2 \right]^{1/2}$$

where $\|f_i\|_p$ is defined as:

$$\|f_i\|_p = \left[\int_0^\infty \omega_i |f_i|^p dt \right]^{1/p}$$

where ω_i is the weighting factor. ω_i is particularly useful for scaling forces and torques of different units.

Definition 5: Let $v(\cdot): L^p_{pe} \rightarrow L^p_{pe}$. We say that the operator $V(\cdot)$ is L^p -stable, if:

- $v(\cdot): L^p_{pe} \rightarrow L^p_{pe}$
- there exist finite real constants α_4 and β_4 such that:

$$\|V(e)\|_p \leq \alpha_4 \|e\|_p + \beta_4 \quad \forall e \in L^p_{pe}$$

According to this definition we first assume that the operator maps L^p_{pe} to L^p_{pe} . It is clear that if one does not show that $v(\cdot): L^p_{pe} \rightarrow L^p_{pe}$, the satisfaction of condition (a) is impossible since L^p_{pe} contains L^p . Once mapping, $v(\cdot)$, from L^p_{pe} to L^p_{pe} is established, then we say that the operator $v(\cdot)$ is L^p -stable if, whenever the input belongs to L^p_{pe} , the resulting output belongs to L^p_{pe} . Moreover, the norm of the output is not larger than α_4 times the norm of the input plus the offset constant β_4 .

Definition 6: The smallest α_4 such that there exist a β_4 so that inequality b of Definition 5 is satisfied is called the gain of the operator $v(\cdot)$.

Definition 7: Let $V(\cdot): L^p_{pe} \rightarrow L^p_{pe}$. The operator $V(\cdot)$ is said to be causal if:

$$V(e)_T = V(e_T) \quad \forall T < \infty \quad \text{and} \quad \forall e \in L^p_{pe}$$

Proof of the Nonlinear Stability Proposition. Define the closed-loop mapping $A: r \rightarrow e$ (Fig. 4).

$$e = r - H(V(e)) \tag{A1}$$

For each finite T , inequality (A2) is true.

$$\|e_T\|_p \leq \|r_T\|_p + \|H(V(e))_T\|_p \quad \text{for all } t \in (0, T) \tag{A2}$$

Since $H(V(e))$ is L^p -stable. Therefore, inequality (A3) is true.

$$\|e_T\|_p \leq \|r_T\|_p + \alpha_5 \alpha_4 \|e_T\|_p + \alpha_5 \beta_4 + \beta_5 \quad \text{for all } t \in (0, T) \tag{A3}$$

Since $\alpha_5 \alpha_4$ is less than unity:

$$\|e_T\|_p \leq \frac{\|r_T\|_p}{1 - \alpha_5 \alpha_4} + \frac{\alpha_5 \beta_4 + \beta_5}{1 - \alpha_5 \alpha_4} \quad \text{for all } t \in (0, T) \tag{A4}$$

Inequality (A4), shows that $e(\cdot)$ is bounded over $(0, T)$. Because this reasoning is valid for every finite T , it follows that $e(\cdot) \in L^p_{pe}$, i.e., that $A: L^p_{pe} \rightarrow L^p_{pe}$. Next we show that the mapping A is L^p -stable in the sense of definition 5. Since $r \in L^p_{pe}$, therefore $\|r_T\|_p < \infty$ for all $t \in (0, \infty)$, therefore in-

equality (A5) is true.

$$\|l\|_p < \infty \quad \text{for all } t \in (0, \infty) \quad (\text{A5})$$

inequality (A5) implies e belongs to L_p -space whenever r belongs to L_p -space. With the same reasoning from equations (A1) to (A5), it can be shown that inequality (A6) is true.

$$\|l\|_p \leq \frac{\|r\|_p}{1 - \alpha_5 \alpha_4} + \frac{\alpha_5 \beta_4 + \beta_5}{1 - \alpha_5 \alpha_4} \quad \text{for all } t \in (0, \infty) \quad (\text{A6})$$

Inequality (A6) shows the linear boundedness of e (condition b of definition 5). Inequalities (A5) and (A6) taken together, guarantee that the closed-loop mapping A is L_p -stable.

APPENDIX B

A very rigid environment generates a very large force for a small displacement. We choose the minimum singular value of E to represent the size of E . The following proposition states the limiting value of the force when the robot manipulator is in contact with a very rigid environment.

If $\sigma_{\min}(E) > M_0$, where M_0 is an arbitrarily large number, then the value of the force given by equation (13) will approach to the expression given by equation (B1)

$$f_{\infty} = (S + GH)^{-1} G r \quad (\text{B1})$$

Proof: We will prove that $|f_{\infty} - f|$ approaches a small number as M_0 approaches a large number.

$$f_{\infty} - f = (S + GH)^{-1} [I_n - (S + GH)^{-1} E (I_n + SE + GHE)^{-1}] G r \quad (\text{B2})$$

Factoring $(I_n + SE + GHE)^{-1}$ to the right-hand side:

$$f_{\infty} - f = (S + GH)^{-1} (I_n + SE + GHE)^{-1} G r \quad (\text{B3})$$

$$|f_{\infty} - f| < \sigma_{\max}(S + GH)^{-1} \times \sigma_{\max}(I_n + SE + GHE)^{-1} \times \sigma_{\max}(G) |r| \quad (\text{B4})$$

$$|f_{\infty} - f| < \frac{\sigma_{\max}(G) |r|}{\sigma_{\min}(S + GH) \times |\sigma_{\min}(SE + GHE) - 1|} \quad (\text{B5})$$

$$|f_{\infty} - f| < \frac{\sigma_{\max}(G) |r|}{\sigma_{\min}(S + GH) \times |\sigma_{\min}(S + GH) \times \sigma_{\min}(E) - 1|} \quad (\text{B6})$$

$\sigma_{\max}(G)$ and $\sigma_{\min}(S + GH)$ are bounded values. If $\sigma_{\min}(E) > M_0$, then it is clear that the left-hand side of inequality (B6) can be an arbitrarily small number by choosing M_0 to be a large number. The proof for $y_{\infty} \approx 0$ is similar to the above.

APPENDIX C

The objective is to find a sufficient condition for stability of the closed-loop system in Fig. 3 by Nyquist Criterion. The block diagram in Fig. 3 can be reduced to the block diagram in Fig. C1 when all the operators are linear transfer function matrices and $x_0 = 0$

There are two elements in the feedback loop; GHE and SE . SE shows the natural force feedback while GHE represents the controlled force feedback in the system. If $H = 0$, then the system in Fig. C1 reduces to the system in Fig. 2 (a stable positioning robot manipulator which is in contact with the environment E). The objective is to use Nyquist Criterion (9) to arrive at the sufficient condition for stability of the system when $H \neq 0$. The following conditions are regarded:

1) The closed loop system in Fig. C1 is stable if $H = 0$. This condition simply states the stability of the robot manipulator and environment when they are in contact. (Fig. 2 shows this configuration.)

2) H is chosen as a stable linear transfer function matrix.

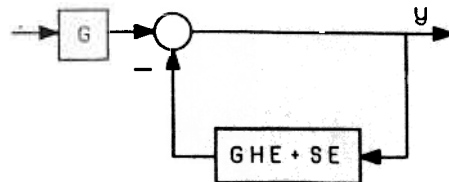


Fig. C1 Simplified block diagram of the system in Fig. 3

Therefore the augmented loop transfer function ($GHE + SE$) has the same number of unstable poles that SE has. Note that in many cases SE is a stable system.

3) Number of poles on $j\omega$ axis for both loop SE and ($GHE + SE$) are equal.

Considering that the system in Fig. C1 is stable when $H = 0$, we plan to find how robust the system is when GHE is added to the feedback loop. If the loop transfer function SE (without compensator, H) develops a stable closed-loop system, then we are looking for a condition on H such that the augmented loop transfer function ($GHE + SE$) guarantees the stability of the closed-loop system. According to the Nyquist Criterion, the system in Fig. C1 remains stable if the anti-clockwise encirclement of the $\det(SE + GHE + I_n)$ around the center of the s -plane is equal to the number of unstable poles of the loop transfer function ($GHE + SE$). According to conditions 2 and 3, the loop transfer functions SE and ($GHE + SE$) both have the same number of unstable poles. The closed-loop system when $H = 0$ is stable according to condition 1; the encirclements of $\det(SE + I_n)$ is equal to unstable poles of SE . When GHE is added to the system, for stability of the closed-loop system, the number of the encirclements of $\det(SE + GHE + I_n)$ must be equal to the number of unstable poles of the ($GHE + SE$). Since the number of unstable poles of ($SE + GHE$) and SE are the same, therefore the stability of the system $\det(SE + GHE + I_n)$ must have the same number of encirclements that $\det(SE + I_n)$ has. A sufficient condition to guarantee the equality of the number of encirclements of $\det(SE + GHE + I_n)$ and $\det(SE + I_n)$ is that the $\det(SE + GHE + I_n)$ does not pass through the origin of the s -plane for all possible nonzero but finite values of H , or

$$\det(SE + GHE + I_n) \neq 0 \quad \text{for all } \omega \in (0, \infty) \quad (\text{C1})$$

If inequality C1 does not hold then there must be a nonzero vector z such that:

$$(SE + GHE + I_n)z = 0 \quad (\text{C2})$$

$$\text{or: } GHE z = -(SE + I_n)z \quad (\text{C3})$$

A sufficient condition to guarantee that equality (C3) will not happen is given by inequality (C4).

$$\sigma_{\max}(GHE) < \sigma_{\min}(SE + I_n) \quad \text{for all } \omega \in (0, \infty) \quad (\text{C4})$$

or a more conservative condition:

$$\sigma_{\max}(H) < \frac{1}{\sigma_{\max}(E(SE + I_n)^{-1}G)} \quad \text{for all } \omega \in (0, \infty) \quad (\text{C5})$$

Note that $E(SE + I_n)^{-1}G$ is the transfer function matrix that maps e to the contact force, f . Figure 4 shows the closed-loop system. According to the result of the proposition, H must be chosen such that the size of H is smaller than the reciprocal of the size of the forward loop transfer function, $E(SE + I_n)^{-1}G$.

APPENDIX D

The following inequalities are true when $p = 2$ and H and V are linear operators.

$$\|H(V(e))\|_p \leq \nu \|V(e)\|_p \quad (\text{D1})$$

$$\|V(e)\|_p \leq \mu \|e\|_p \quad (\text{D2})$$

where:

$\mu = \sigma_{\max}(Q)$, and Q is the matrix whose ij th entry is given by $(Q)_{ij} = \sup_{\omega} |(V)_{ij}|$,

$\nu = \sigma_{\max}(R)$, and R is the matrix whose ij th entry is given by $(R)_{ij} = \sup_{\omega} |(H)_{ij}|$

Substituting inequality (D2) in (D1):

$$\|HV(e)\|_p \leq \mu \nu \|e\|_p \quad (D3)$$

According to the stability condition, to guarantee the closed loop stability $\mu \nu < 1$ or:

$$\nu < \frac{1}{\mu} \quad (D4)$$

Note that the followings are true:

$$\sigma_{\max}(V) \leq \mu \quad \text{for all } \omega \in (0, \infty) \quad (D5)$$

$$\sigma_{\max}(H) \leq \nu \quad \text{for all } \omega \in (0, \infty) \quad (D6)$$

Substituting (D5) and (D6) into inequality (D4) which guarantees the stability of the system, the following inequality is obtained:

$$\sigma_{\max}(H) < \frac{1}{\sigma_{\max}(V)} \quad \text{for all } \omega \in (0, \infty) \quad (D7)$$

$$\sigma_{\max}(H) < \frac{1}{\sigma_{\max}(E(I_n + SE)^{-1}G)} \quad \text{for all } \omega \in (0, \infty) \quad (D8)$$

Inequality (D8) is identical to inequality (26). This shows that the linear condition for stability given by the multivariable Nyquist Criterion is a subset of the general condition given by the Small Gain Theorem.

APPENDIX E

This Appendix is dedicated to deriving of the Jacobian and the mass matrix of a general five-bar linkage. In Fig. E1, J_i , l_i , x_i , m_i , and θ_i represent the moment of the inertia relative to the end-point, length, location of the center of mass, mass and the orientation of each link for $i = 1, 2, 3$ and 4.

Using the standard method, the Jacobian of the linkage can be represented by equation (E1).

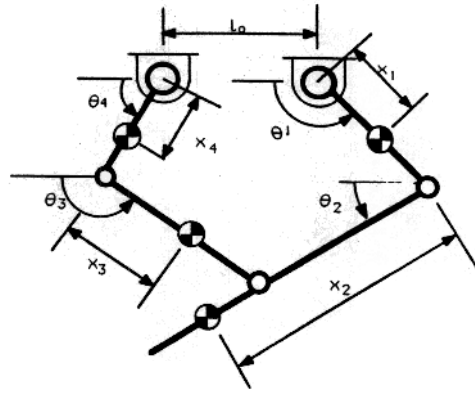


Fig. E1 The five bar linkage in the general form

$$J_c = \begin{bmatrix} J_{11} & J_{12} \\ J_{21} & J_{22} \end{bmatrix} \quad (E1)$$

where:

$$J_{11} = -l_1 \sin(\theta_1) + a l_5 \sin(\theta_2), \quad J_{21} = l_1 \cos(\theta_1) - a l_5 \cos(\theta_2)$$

$$J_{12} = b l_5 \sin(\theta_2), \quad J_{22} = b l_5 \cos(\theta_2)$$

The mass matrix is given by equation (E2).

$$M = \begin{bmatrix} M_{11} & M_{12} \\ M_{21} & M_{22} \end{bmatrix} \quad (E2)$$

where:

$$M_{11} = J_1 + m_2 l_1^2 + J_2 a^2 + J_3 c^2 + 2 x_2 l_1 \cos(\theta_1 - \theta_2) a m_2$$

$$M_{12} = J_2 a b + b \cos(\theta_1 - \theta_2) x_2 l_1 m_2 + J_3 c d$$

$$+ c \cos(\theta_4 - \theta_3) x_3 l_4 m_3$$

$$M_{21} = M_{12}$$

$$M_{22} = 2 m_3 l_4 x_3 d \cos(\theta_4 - \theta_3) + J_3 d^2 + J_4 + m^3 l_4^2 + J_2 b^2$$

a, b, c, d are given below.

$$a = l_1 \sin(\theta_1 - \theta_3) / (l_2 \sin(\theta_2 - \theta_3))$$

$$b = l_4 \sin(\theta_4 - \theta_3) / (l_2 \sin(\theta_2 - \theta_3))$$

$$c = l_1 \sin(\theta_1 - \theta_2) / (l_3 \sin(\theta_2 - \theta_3))$$

$$d = l_4 \sin(\theta_1 - \theta_2) / (l_3 \sin(\theta_2 - \theta_3))$$

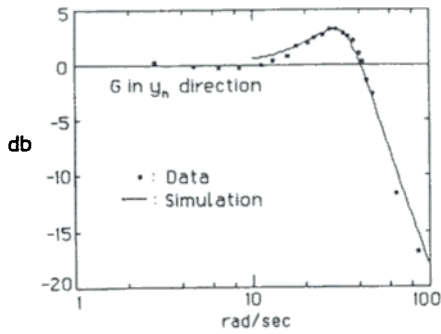


Fig. 9 The position transfer function, G

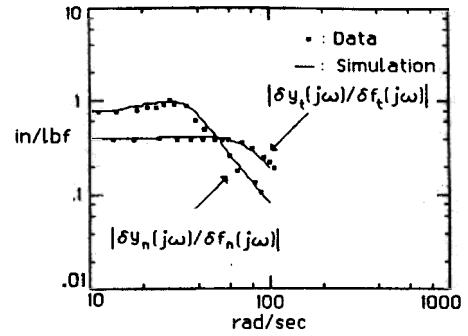


Fig. 11 The end-point admittance (1/impedance)

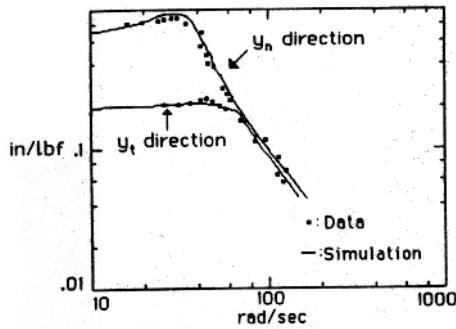


Fig. 10 The sensitivity transfer function, S

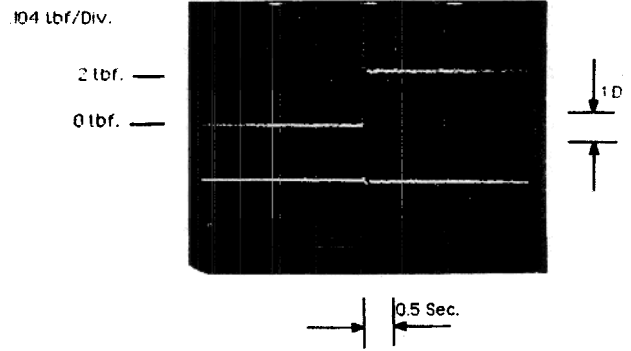


Fig. 12 Force in the y_n -direction increases from zero to 2 lbf

the input command represents the magnitude of G at each frequency. For measurement of the sensitivity transfer function matrix, the input excitation was supplied by the rotation of an eccentric mass mounted on the tool bit. The rotating mass exerts a centrifugal, sinusoidal force on the tool bit. The frequency of the imposed force is equal to the frequency of rotation of the mass. By varying the frequency of the rotation of the mass, one can vary the frequency of the imposed force on the end-effector. Figure 10 depicts the sensitivity transfer function. The values of the sensitivity transfer functions along the normal and tangential directions, within their bandwidths, are 0.7 in/lbf and 0.197 in/lbf, respectively.

The nature of compliancy for the end effector is given by equation (31). H was chosen such that $(S+H)^{-1}$ in each direction is equal to the desired stiffness. H must also guarantee the stability of the closed-loop system. The stability criteria for a one-degree-of-freedom system is given by inequalities 32 and 33. Inequality 33 shows that the more rigid the environment is, the smaller H must be chosen to guarantee the stability of the closed-loop system. In the case of a rigid environment ("large" E) and a "good" positioning system ("small" S), H must be chosen as a very small gain. The values for H along the normal and tangential directions within their bandwidths are 0.01 in/lbf and 0.194 in/lbf, respectively. These values result in 0.39 in/lbf and 0.7 in/lbf for $(S+H)$ within the bandwidth of the system. Figure 11 shows the experimental and theoretical values of the end-point compliancy (Fig. 11 actually shows the end-point admittance where it is reciprocal of the impedance in the linear case.)

In another set of experiments, the whole end-effector was moved in two different directions to encounter an edge of a part. The objective was to observe the uncoupled time-domain dynamic behavior of the end-effector when the end-effector is in contact with the hard environment. The controller was designed such that the values of $(S+H)^{-1}$ in tangential and normal direction are 0.32 lbf/in and 4.0 lb/in, respectively. First the end-effector was moved 0.5 in. beyond the edge of the part in y_n -direction. Figure 12 shows the contact forces. The force in y_n -direction increases from zero to 2.0 lbf while

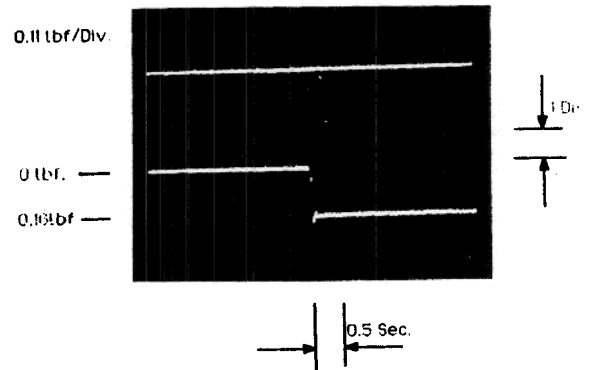


Fig. 13 Force in the y_t -direction increases from zero to 0.16 lb

the force in the y_t -direction remains at zero. Next the end-effector was moved 0.5 in. beyond the edge of the part in the y_t -direction. Figure 13 shows the contact forces. The force in y_t -direction increases from zero to 0.16 lbf while the force in y_n -direction remains at zero. In both cases the end-effector was moved as 0.5 in. beyond the edge of the stiff wall. Since the stiffness of the end-effector in y_n -direction is larger than the stiffness in y_t -direction, the contact force in y_n -direction is larger than the contact force in y_t -direction.

11 Summary and Conclusion

A new controller architecture for compliance control has been investigated using unstructured models for dynamic behavior of robot manipulators and environment. This unified approach of modeling robot and environment dynamics is expressed in terms of sensitivity functions. The control approach allows not only for tracking the input-command vector, but also for compliancy in the constrained maneuverings. An active end-effector has been designed, built, and tested for verification of the control method. The active end-effector (unlike the passive system) does not con-

tain any spring or dampers. The compliancy in the active end-effector is developed electronically and therefore can be modulated by an on-line computer. Satisfying a kinematic constraint for this end-effector allows for uncoupled dynamic behavior for a bounded range. Two state-of-the-art miniature actuators power the end-effector directly. A miniature force cell measures the forces in two dimensions. The tool holder can maneuver a very light pneumatic grinder in a linear workspace of about 0.3×0.3 in. A bound for the global stability of the manipulator and environment has been derived. For stability of the environment and the robot taken as a whole, there must be some initial compliancy either in the robot or in the environment. The initial compliancy in the robot can be obtained by a nonzero sensitivity function for the positioning controller or a passive compliant element.

Acknowledgment

This research work is supported by the National Science Foundation grant under Contract NSF/DMC-8604123.

References

- Hogan, N., "Impedance Control: An Approach to Manipulation," *ASME JOURNAL OF DYNAMIC SYSTEMS, MEASUREMENT, AND CONTROL*, Vol. 107, 1985.
- Hollis, R. L., "A Planar XY Robotic Fine Positioning Device," *IEEE International Conference on Robotics and Automation*, St. Louis, MO, Mar. 1985.
- Kazerooni, H., and Houpt, P. K., "On The Loop Transfer Recovery," *Int. J. of Control*, Vol. 43, No. 3, Mar. 1986.
- Kazerooni, H., "Fundamentals of Robust Compliant Motion for Manipulators," *IEEE J. of Robotics and Automation*, Vol. 2, No. 2, June 1986.
- Kazerooni, H., "A Design Method for Robust Compliant Motion of Manipulators," *IEEE J. of Robotics and Automation*, Vol. 2, No. 2, June 1986.
- Kazerooni, "An Approach to Automated Deburring by Robot Manipulators," *ASME JOURNAL OF DYNAMIC SYSTEMS, MEASUREMENT, AND CONTROL*, Dec. 1986.
- Kazerooni, H., "Robotic Deburring of Parts with Unknown Geometry," *Proceedings of American Control Conference*, Atlanta, GA, June 1988.
- Kazerooni, H., "Direct Drive Active Compliant End-effector," *IEEE J. of Robotics and Automation*, Vol. 4, No. 3, June 1988.
- Lehtomaki, N. A., Sandell, N. R., and Athans, M., "Robustness Results in Linear-Quadratic Gaussian Based Multivariable Control Designs," *IEEE Trans. on Automatic Control*, Vol. 26, No. 1, Feb. 1981, pp. 75-92.
- Mason, M. T., "Compliance and Force Control for Computer Controlled Manipulators," *IEEE Transaction on Systems, Man, and Cybernetics*, SMC-11(6), June 1981, pp. 418-432.
- Paul, R. P. C., and Shimano, B., "Compliance and Control," *Proceedings of the Joint Automatic Control Conference*, San Francisco, 1976, pp. 694-699.
- Raibert, M. H., and Craig, J. J., "Hybrid Position/Force Control of Manipulators," *ASME JOURNAL OF DYNAMIC SYSTEMS, MEASUREMENT, AND CONTROL*, Vol. 102, June 1981, pp. 126-133.
- Salisbury, K. J., "Active Stiffness Control of Manipulator in Cartesian Coordinates," *Proceedings of the 19th IEEE Conference on Decision and Control*, pp. 95-100, IEEE, Albuquerque, N. Mex., Dec. 1980.
- Slotine, J. J., "The Robust Control of Robot Manipulators," *The International J. of Robotics Research*, Vol. 4, No. 2, 1985.
- Vidyasagar, M., *Nonlinear Systems Analysis*, Prentice-Hall, 1978.
- Vidyasagar, M., and Desoer, C. A., *Feedback Systems: Input-Output Properties*, Academic Press, 1975.
- Vidyasagar, M., Spong, M. W., "Robust Nonlinear Control of Robot Manipulators," *IEEE Conference on Decision and Control*, Dec. 1985.
- Whitney, D. E., "Force-Feedback Control of Manipulator Fine Motions," *ASME JOURNAL OF DYNAMIC SYSTEMS, MEASUREMENT, AND CONTROL*, June 1977, pp. 91-97.
- Yoshikawa, T., "Dynamic Manipulability of Robot Manipulators," *Journal of Robotic Systems*, Vol. 2, No. 1, 1985.

APPENDIX A

Definitions 1 to 7 will be used in the stability proof of the closed-loop system (Vidyasagar, 1978, Vidyasagar and Desoer, 1975).

Definition 1: For all $p \in (1, \infty)$, we label as L_p^n the set con-

sisting of all functions $f = (f_1, f_2, \dots, f_n)^T: (0, \infty) \rightarrow R^n$ such that:

$$\int_0^\infty |f_i|^p dt < \infty \quad \text{for } i = 1, 2, \dots, n$$

Definition 2: For all $T \in (0, \infty)$, the function f_T defined by:

$$f_T = \begin{cases} f & 0 \leq t \leq T \\ 0 & T < t \end{cases}$$

is called the truncation of f to the interval $(0, T)$.

Definition 3: The set of all functions $f = (f_1, f_2, \dots, f_n)^T: ((0, \infty) \rightarrow R^n$ such that $f^T \in L_p^n$ for all finite T is denoted by L_{pe}^n . f by itself may or may not belong to L_p^n .

Definition 4: The norm on L_p^n is defined by:

$$\|f\|_p = \left[\sum_{i=1}^n \|f_i\|_p^2 \right]^{1/2}$$

where $\|f_i\|_p$ is defined as:

$$\|f_i\|_p = \left[\int_0^\infty \omega_i |f_i|^p dt \right]^{1/p}$$

where ω_i is the weighting factor. ω_i is particularly useful for scaling forces and torques of different units.

Definition 5: Let $v(\cdot): L_{pe}^n \rightarrow L_{pe}^n$. We say that the operator $V(\cdot)$ is L_p -stable, if:

- $v(\cdot): L_{pe}^n \rightarrow L_{pe}^n$
- there exist finite real constants α_4 and β_4 such that:

$$\|V(e)\|_p \leq \alpha_4 \|e\|_p + \beta_4 \quad \forall e \in L_{pe}^n$$

According to this definition we first assume that the operator maps L_{pe}^n to L_{pe}^n . It is clear that if one does not show that $v(\cdot): L_{pe}^n \rightarrow L_{pe}^n$, the satisfaction of condition (a) is impossible since L_{pe}^n contains L_p^n . Once mapping, $v(\cdot)$, from L_{pe}^n to L_{pe}^n is established, then we say that the operator $v(\cdot)$ is L_p -stable if, whenever the input belongs to L_p^n , the resulting output belongs to L_p^n . Moreover, the norm of the output is not larger than α_4 times the norm of the input plus the offset constant β_4 .

Definition 6: The smallest α_4 such that there exist a β_4 so that inequality b of Definition 5 is satisfied is called the gain of the operator $v(\cdot)$.

Definition 7: Let $V(\cdot): L_{pe}^n \rightarrow L_{pe}^n$. The operator $V(\cdot)$ is said to be causal if:

$$V(e)_T = V(e_T) \quad \forall T < \infty \quad \text{and} \quad \forall e \in L_{pe}^n$$

Proof of the Nonlinear Stability Proposition. Define the closed-loop mapping $A: r \rightarrow e$ (Fig. 4).

$$e = r - H(V(e)) \quad (A1)$$

For each finite T , inequality (A2) is true.

$$\|e_T\|_p \leq \|r_T\|_p + \|H(V(e))_T\|_p \quad \text{for all } t \in (0, T) \quad (A2)$$

Since $H(V(e))$ is L_p -stable. Therefore, inequality (A3) is true.

$$\|e_T\|_p \leq \|r_T\|_p + \alpha_5 \alpha_4 \|e_T\|_p + \alpha_5 \beta_4 + \beta_5 \quad \text{for all } t \in (0, T) \quad (A3)$$

Since $\alpha_5 \alpha_4$ is less than unity:

$$\|e_T\|_p \leq \frac{\|r_T\|_p}{1 - \alpha_5 \alpha_4} + \frac{\alpha_5 \beta_4 + \beta_5}{1 - \alpha_5 \alpha_4} \quad \text{for all } t \in (0, T) \quad (A4)$$

Inequality (A4), shows that $e(\cdot)$ is bounded over $(0, T)$. Because this reasoning is valid for every finite T , it follows that $e(\cdot) \in L_{pe}^n$, i.e., that $A: L_{pe}^n \rightarrow L_{pe}^n$. Next we show that the mapping A is L_p -stable in the sense of definition 5. Since $r \in L_p^n$, therefore $\|r\|_p < \infty$ for all $t \in (0, \infty)$, therefore in-

equality (A5) is true.

$$\|e\|_p < \infty \quad \text{for all } t \in (0, \infty) \quad (\text{A5})$$

inequality (A5) implies e belongs to L_p -space whenever r belongs to L_p -space. With the same reasoning from equations (A1) to (A5), it can be shown that inequality (A6) is true.

$$\|e\|_p \leq \frac{\|r\|_p}{1 - \alpha_5 \alpha_4} + \frac{\alpha_5 \beta_4 + \beta_5}{1 - \alpha_5 \alpha_4} \quad \text{for all } t \in (0, \infty) \quad (\text{A6})$$

Inequality (A6) shows the linear boundedness of e (condition b of definition 5). Inequalities (A5) and (A6) taken together, guarantee that the closed-loop mapping A is L_p -stable.

APPENDIX B

A very rigid environment generates a very large force for a small displacement. We choose the minimum singular value of E to represent the size of E . The following proposition states the limiting value of the force when the robot manipulator is in contact with a very rigid environment.

If $\sigma_{\min}(E) > M_0$, where M_0 is an arbitrarily large number, then the value of the force given by equation (13) will approach to the expression given by equation (B1)

$$f_\infty = (S + GH)^{-1} G r \quad (\text{B1})$$

Proof: We will prove that $|f_\infty - f|$ approaches a small number as M_0 approaches a large number.

$$f_\infty - f = (S + GH)^{-1} [I_n - (S + GH) E (I_n + SE + GHE)^{-1}] G r \quad (\text{B2})$$

Factoring $(I_n + SE + GHE)^{-1}$ to the right-hand side:

$$f_\infty - f = (S + GH)^{-1} (I_n + SE + GHE)^{-1} G r \quad (\text{B3})$$

$$|f_\infty - f| < \sigma_{\max}(S + GH)^{-1} \times \sigma_{\max}(I_n + SE + GHE)^{-1} \times \sigma_{\max}(G) |r| \quad (\text{B4})$$

$$|f_\infty - f| < \frac{\sigma_{\max}(G) |r|}{\sigma_{\min}(S + GH) \times |\sigma_{\min}(SE + GHE) - 1|} \quad (\text{B5})$$

$$|f_\infty - f| < \frac{\sigma_{\max}(G) |r|}{\sigma_{\min}(S + GH) \times |\sigma_{\min}(S + GH) \times \sigma_{\min}(E) - 1|} \quad (\text{B6})$$

$\sigma_{\max}(G)$ and $\sigma_{\min}(S + GH)$ are bounded values. If $\sigma_{\min}(E) > M_0$, then it is clear that the left-hand side of inequality (B6) can be an arbitrarily small number by choosing M_0 to be a large number. The proof for $y_\infty \approx 0$ is similar to the above.

APPENDIX C

The objective is to find a sufficient condition for stability of the closed-loop system in Fig. 3 by Nyquist Criterion. The block diagram in Fig. 3 can be reduced to the block diagram in Fig. C1 when all the operators are linear transfer function matrices and $x_0 = 0$

There are two elements in the feedback loop; GHE and SE . SE shows the natural force feedback while GHE represents the controlled force feedback in the system. If $H = 0$, then the system in Fig. C1 reduces to the system in Fig. 2 (a stable positioning robot manipulator which is in contact with the environment E). The objective is to use Nyquist Criterion (9) to arrive at the sufficient condition for stability of the system when $H \neq 0$. The following conditions are regarded:

1) The closed loop system in Fig. C1 is stable if $H = 0$. This condition simply states the stability of the robot manipulator and environment when they are in contact. (Fig. 2 shows this configuration.)

2) H is chosen as a stable linear transfer function matrix.

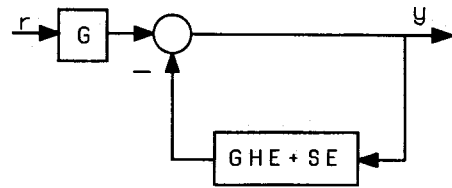


Fig. C1 Simplified block diagram of the system in Fig. 3

Therefore the augmented loop transfer function ($GHE + SE$) has the same number of unstable poles that SE has. Note that in many cases SE is a stable system.

3) Number of poles on $j\omega$ axis for both loop SE and ($GHE + SE$) are equal.

Considering that the system in Fig. C1 is stable when $H = 0$, we plan to find how robust the system is when GHE is added to the feedback loop. If the loop transfer function SE (without compensator, H) develops a stable closed-loop system, then we are looking for a condition on H such that the augmented loop transfer function ($GHE + SE$) guarantees the stability of the closed-loop system. According to the Nyquist Criterion, the system in Fig. C1 remains stable if the anti-clockwise encirclement of the $\det(SE + GHE + I_n)$ around the center of the s -plane is equal to the number of unstable poles of the loop transfer function ($GHE + SE$). According to conditions 2 and 3, the loop transfer functions SE and ($GHE + SE$) both have the same number of unstable poles. The closed-loop system when $H = 0$ is stable according to condition 1; the encirclements of $\det(SE + I_n)$ is equal to unstable poles of SE . When GHE is added to the system, for stability of the closed-loop system, the number of the encirclements of $\det(SE + GHE + I_n)$ must be equal to the number of unstable poles of the ($GHE + SE$). Since the number of unstable poles of ($SE + GHE$) and SE are the same, therefore the stability of the system $\det(SE + GHE + I_n)$ must have the same number of encirclements that $\det(SE + I_n)$ has. A sufficient condition to guarantee the equality of the number of encirclements of $\det(SE + GHE + I_n)$ and $\det(SE + I_n)$ is that the $\det(SE + GHE + I_n)$ does not pass through the origin of the s -plane for all possible nonzero but finite values of H , or

$$\det(SE + GHE + I_n) \neq 0 \quad \text{for all } \omega \in (0, \infty) \quad (\text{C1})$$

If inequality C1 does not hold then there must be a nonzero vector z such that:

$$(SE + GHE + I_n)z = 0 \quad (\text{C2})$$

$$\text{or: } GHE z = -(SE + I_n)z \quad (\text{C3})$$

A sufficient condition to guarantee that equality (C3) will not happen is given by inequality (C4).

$$\sigma_{\max}(GHE) < \sigma_{\min}(SE + I_n) \quad \text{for all } \omega \in (0, \infty) \quad (\text{C4})$$

or a more conservative condition:

$$\sigma_{\max}(H) < \frac{1}{\sigma_{\max}(E(SE + I_n)^{-1}G)} \quad \text{for all } \omega \in (0, \infty) \quad (\text{C5})$$

Note that $E(SE + I_n)^{-1}G$ is the transfer function matrix that maps e to the contact force, f . Figure 4 shows the closed-loop system. According to the result of the proposition, H must be chosen such that the size of H is smaller than the reciprocal of the size of the forward loop transfer function, $E(SE + I_n)^{-1}G$.

APPENDIX D

The following inequalities are true when $p = 2$ and H and V are linear operators.

$$\|H(V(e))\|_p \leq \nu \|V(e)\|_p \quad (\text{D1})$$

$$\|V(e)\|_p \leq \mu \|e\|_p \quad (\text{D2})$$

where:

$\mu = \sigma_{\max}(Q)$, and Q is the matrix whose ij th entry is given by $(Q)_{ij} = \sup_{\omega} |(V)_{ij}|$,

$\nu = \sigma_{\max}(R)$, and R is the matrix whose ij th entry is given by $(R)_{ij} = \sup_{\omega} |(H)_{ij}|$

Substituting inequality (D2) in (D1):

$$\|HV(e)\|_p \leq \mu \nu \|e\|_p \quad (D3)$$

According to the stability condition, to guarantee the closed loop stability $\mu\nu < 1$ or:

$$\nu < \frac{1}{\mu} \quad (D4)$$

Note that the followings are true:

$$\sigma_{\max}(V) \leq \mu \quad \text{for all } \omega \in (0, \infty) \quad (D5)$$

$$\sigma_{\max}(H) \leq \nu \quad \text{for all } \omega \in (0, \infty) \quad (D6)$$

Substituting (D5) and (D6) into inequality (D4) which guarantees the stability of the system, the following inequality is obtained:

$$\sigma_{\max}(H) < \frac{1}{\sigma_{\max}(V)} \quad \text{for all } \omega \in (0, \infty) \quad (D7)$$

$$\sigma_{\max}(H) < \frac{1}{\sigma_{\max}(E(I_n + SE)^{-1}G)} \quad \text{for all } \omega \in (0, \infty) \quad (D8)$$

Inequality (D8) is identical to inequality (26). This shows that the linear condition for stability given by the multivariable Nyquist Criterion is a subset of the general condition given by the Small Gain Theorem.

APPENDIX E

This Appendix is dedicated to deriving of the Jacobian and the mass matrix of a general five-bar linkage. In Fig. E1, J_i , l_i , x_i , m_i , and θ_i represent the moment of the inertia relative to the end-point, length, location of the center of mass, mass and the orientation of each link for $i=1, 2, 3$ and 4.

Using the standard method, the Jacobian of the linkage can be represented by equation (E1).

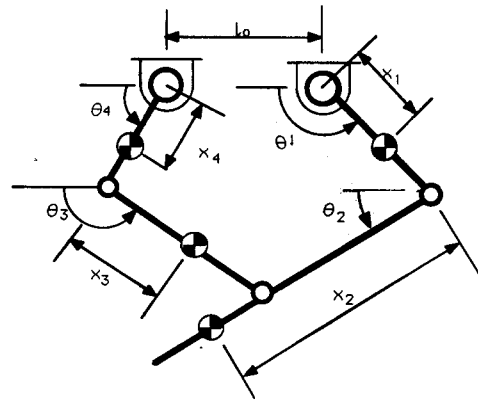


Fig. E1 The five bar linkage in the general form

$$J_c = \begin{bmatrix} J_{11} & J_{12} \\ J_{21} & J_{22} \end{bmatrix} \quad (E1)$$

where:

$$J_{11} = -l_1 \sin(\theta_1) + a l_5 \sin(\theta_2), \quad J_{21} = l_1 \cos(\theta_1) - a l_5 \cos(\theta_2)$$

$$J_{12} = b l_5 \sin(\theta_2), \quad J_{22} = b l_5 \cos(\theta_2)$$

The mass matrix is given by equation (E2).

$$M = \begin{bmatrix} M_{11} & M_{12} \\ M_{21} & M_{22} \end{bmatrix} \quad (E2)$$

where:

$$M_{11} = J_1 + m_2 l_1^2 + J_2 a^2 + J_3 c^2 + 2 x_2 l_1 \cos(\theta_1 - \theta_2) a m_2$$

$$M_{12} = J_2 a b + b \cos(\theta_1 - \theta_2) x_2 l_1 m_2 + J_3 c d$$

$$+ c \cos(\theta_4 - \theta_3) x_3 l_4 m_3$$

$$M_{21} = M_{12}$$

$$M_{22} = 2 m_3 l_4 x_3 d \cos(\theta_4 - \theta_3) + J_3 d^2 + J_4 + m^3 l_4^2 + J_2 b^2$$

a, b, c, d are given below.

$$a = l_1 \sin(\theta_1 - \theta_3) / (l_2 \sin(\theta_2 - \theta_3))$$

$$b = l_4 \sin(\theta_4 - \theta_3) / (l_2 \sin(\theta_2 - \theta_3))$$

$$c = l_1 \sin(\theta_1 - \theta_2) / (l_3 \sin(\theta_2 - \theta_3))$$

$$d = l_4 \sin(\theta_1 - \theta_2) / (l_3 \sin(\theta_2 - \theta_3))$$

$$\beta = 10, \xi = 6.0, \Gamma = 1.0$$

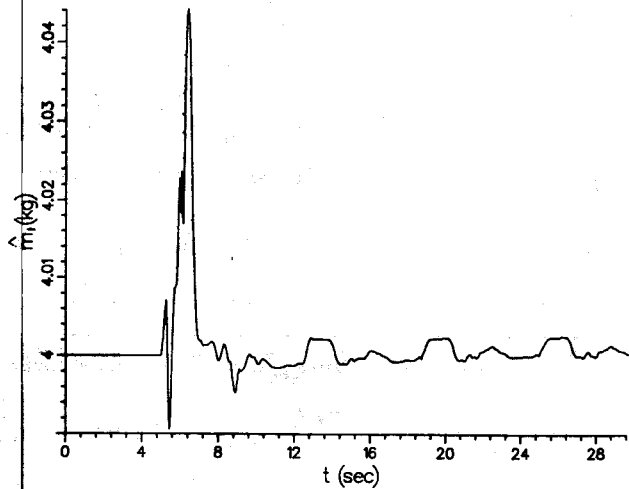


Fig. 5

All parameters were initially assumed to be set to their true value, but the value of mass at the end of the second link, m_2 , was increased from 2 kg to 3 kg at the time $t = 5$ sec. Figures 3 to 6 show the results of the tracking error response and the parameter identification process. $\Gamma_{33} = I$ was used for all the cases shown. Note that the state variables (Figs. 3, 4) have essentially come to their correct values within three seconds. As expected, the estimates of the second mass (Fig. 6) show the most severe estimation errors; however this estimate has also converged to the actual mass value after three seconds. The estimate of the first mass (Fig. 5) shows a maximum error of approximately 10 percent from the actual value.

5 Conclusions

From the above developments, we can draw the following conclusions. First, the adaptive pure computed torque algorithm is easy to implement, computationally very efficient and is stable under moderate feedback gains. The algorithm allows accurate estimations of system parameters and excellent control of the system state variables. The design is made very simple by the explicit expression of the parameter range allowed for stability. Second, if no additional filters are used, and a Lyapunov function method is assumed, then this paper seems to have accounted for many of the reasonable choices of the control laws of the form (5) and adaptation laws in the form of (9).

$$\beta = 10, \xi = 6.0, \Gamma = 1.0$$

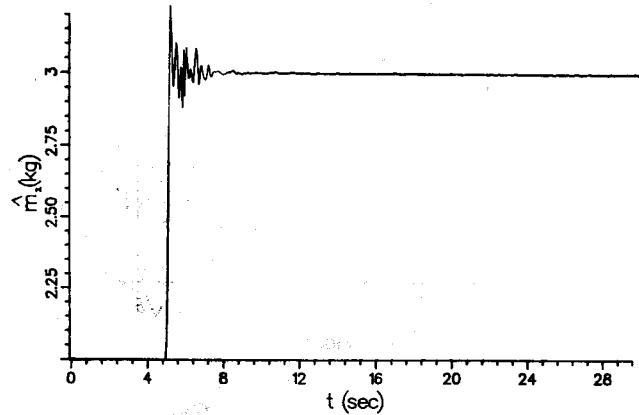


Fig. 6

References

- Craig, J. J., 1986, *Introduction to Robotics: Mechanics and Control*, Addison-Wesley, Reading, Mass.
- Craig, J. J., Hsu, P., and Sastry, S. S., 1987, "Adaptive Control of Mechanical Manipulators," *Int. J. Robotics Research*, Vol. 6, No. 2, pp. 16-28.
- Dubowsky, S., and DesForges, D. T., 1979, "The Application of Model-Referenced Adaptive Control to Robotic Manipulators," *ASME JOURNAL OF DYNAMIC SYSTEMS, MEASUREMENT AND CONTROL*, Vol. 101, pp. 193-200.
- Horowitz, R., and Tomizuka, M., 1980, "An Adaptive Control Scheme for Mechanical Manipulators—Compensation of Nonlinearity and Decoupling Control," *ASME Paper 80-WA/DSC-6*.
- Hsu, P., Bodson, M., Sastry, S., and Paden, B., 1987, "Adaptive Identification and Control for Manipulators without Using Joint Accelerations," *IEEE International Conference on Robotics and Automation*, 1987, pp. 1210-1215.
- Khosla, P., and Kanade, T., 1985, "Parameter Identification of Robot Dynamics," *IEEE Conf. Decision and Control*, Fort Lauderdale, Fla.
- Lee, C. S. G., and Chung, M. J., 1984, "An Adaptive Control Strategy for Mechanical Manipulator," *IEEE Trans. Automatic Control*, Vol. AC-29, No. 9.
- Luh, J. Y. S., Walker, M. W., and Paul, R. P. C., 1980, "On-Line Computational Scheme for Mechanical Manipulators," *ASME JOURNAL OF DYNAMIC SYSTEMS, MEASUREMENT AND CONTROL*, Vol. 1, pp. 60-70.
- Middleton, R. H., and Goodwin, G. C., "Adaptive Computed Torque Control for Rigid Link Manipulators," *Proc. 25th Conf. Doc. Contr.*, Athens, Greece, pp. 68-73.
- Orin, D. E., McGhee, R. B., Vukobratovic, M., and Hartock, G., 1979, "Kinematic and Kinetic Analysis of Open-Chain Linkage Utilizing Newton-Euler Methods," *Mathematical Biosciences*, Vol. 43, pp. 107-130.
- Paul, R. P., 1981, *Robot Manipulators: Mathematics, Programming, and Control*, MIT Press, Cambridge, MA.
- Sadegh, N., and Horowitz, R., 1987, "Stability Analysis of an Adaptive Controller for Robotic Manipulators," *IEEE International Conference on Robotics and Automation*, pp. 1223-1229.
- Slotine, J. J. E., and Li, W., 1987, "On the Adaptive Control of Robot Manipulators," *Int. J. Robotics Research*, Vol. 6, No. 3, pp. 49-59.
- Wang, T., and Kohli, D., 1985, "Closed and Expanded Form of Manipulator Dynamics Using Lagrangian Approach," *ASME Journal of Mechanisms, Transmissions, and Automation in Design*, Vol. 107, pp. 223-225.